

# Generalizing Importance Weighting to A Universal Solver for Distribution Shift Problems

Tongtong Fang<sup>1</sup>    Nan Lu<sup>2</sup>    Gang Niu<sup>3</sup>    Masashi Sugiyama<sup>3,1</sup>

<sup>1</sup>The University of Tokyo    <sup>2</sup>University of Tübingen    <sup>3</sup>RIKEN

## Abstract

*Distribution shift* (DS) may have two levels: the distribution itself changes, and the *support* (i.e., the set where the probability density is non-zero) also changes. When considering the support change between the training and test distributions, there can be four cases: (i) they exactly match; (ii) the training support is wider (and thus covers the test support); (iii) the test support is wider; (iv) they partially overlap. Existing methods are good at cases (i) and (ii), while cases (iii) and (iv) are more common nowadays but still under-explored. In this paper, we generalize *importance weighting* (IW), a golden solver for cases (i) and (ii), to a universal solver for all cases. Specifically, we first investigate why IW may fail in cases (iii) and (iv); based on the findings, we propose *generalized IW* (GIW) that could handle cases (iii) and (iv) and would reduce to IW in cases (i) and (ii). In GIW, the test support is split into an *in-training* (IT) part and an *out-of-training* (OOT) part, and the *expected risk* is decomposed into a weighted classification term over the IT part and a standard classification term over the OOT part, which guarantees the *risk consistency* of GIW. Then, the implementation of GIW consists of three components: (a) the split of validation data is carried out by the one-class support vector machine, (b) the first term of the *empirical risk* can be handled by any IW algorithm given training data and IT validation data, and (c) the second term just involves OOT validation data. Experiments demonstrate that GIW is a universal solver for DS problems, outperforming IW methods in cases (iii) and (iv).

## 1 Introduction

Deep *supervised classification* has been successful where the training and test data should come from the same distribution (Goodfellow et al., 2016). When this assumption does not hold in practice, we suffer from *distribution shift* (DS) problems and the learned classifier may often generalize poorly (Quionero-Candela et al., 2009; Pan and Yang, 2009; Sugiyama and Kawanabe, 2012). Let  $\mathbf{x}$  and  $y$  be the instance (i.e., input) and class-label (i.e., output) random variables. Then, DS means that the *underlying joint density* of the training data  $p_{\text{tr}}(\mathbf{x}, y)$  differs from that of the test data  $p_{\text{te}}(\mathbf{x}, y)$ .

There are two levels in the DS research. At the first level, only the change of the data distribution is considered. With additional assumptions, DS can be reduced into covariate shift  $p_{\text{tr}}(\mathbf{x}) \neq p_{\text{te}}(\mathbf{x})$ , class-prior shift  $p_{\text{tr}}(y) \neq p_{\text{te}}(y)$ , class-posterior shift  $p_{\text{tr}}(y | \mathbf{x}) \neq p_{\text{te}}(y | \mathbf{x})$ , and class-conditional shift  $p_{\text{tr}}(\mathbf{x} | y) \neq p_{\text{te}}(\mathbf{x} | y)$  (Quionero-Candela et al., 2009). We focus on joint shift  $p_{\text{tr}}(\mathbf{x}, y) \neq$

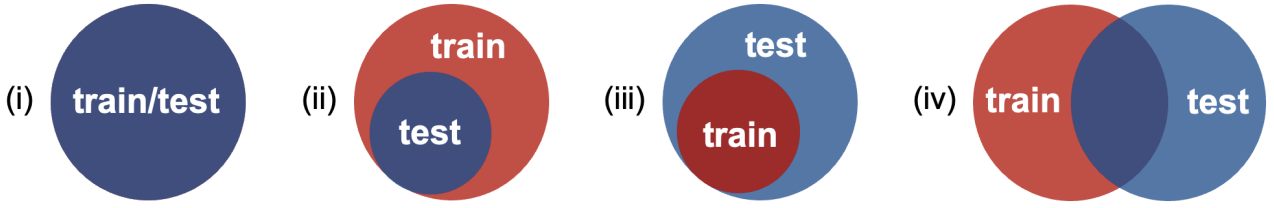


Figure 1: An illustration of the relationship between the training support and the test support.

$p_{te}(\mathbf{x}, y)$ , as it is the most general and difficult case of DS. At the second level, the change of the *support* of the data distribution is also considered, where given any joint density  $p(\mathbf{x}, y)$ , its support is defined as the set  $\{(\mathbf{x}, y) : p(\mathbf{x}, y) > 0\}$ . More specifically, denote by  $\mathcal{S}_{tr}$  and  $\mathcal{S}_{te}$  the support of  $p_{tr}(\mathbf{x}, y)$  and  $p_{te}(\mathbf{x}, y)$ , respectively. When considering the relationship between  $\mathcal{S}_{tr}$  and  $\mathcal{S}_{te}$ , there can be four cases:

- (i)  $\mathcal{S}_{tr}$  and  $\mathcal{S}_{te}$  exactly match, i.e.,  $\mathcal{S}_{tr} = \mathcal{S}_{te}$ ;
- (ii)  $\mathcal{S}_{tr}$  is wider and covers  $\mathcal{S}_{te}$ , i.e.,  $\mathcal{S}_{tr} \supset \mathcal{S}_{te}$  and  $\mathcal{S}_{tr} \setminus \mathcal{S}_{te} \neq \emptyset$ ;
- (iii)  $\mathcal{S}_{te}$  is wider and covers  $\mathcal{S}_{tr}$ , i.e.,  $\mathcal{S}_{tr} \subset \mathcal{S}_{te}$  and  $\mathcal{S}_{te} \setminus \mathcal{S}_{tr} \neq \emptyset$ ;
- (iv)  $\mathcal{S}_{tr}$  and  $\mathcal{S}_{te}$  partially overlap, i.e.,  $\mathcal{S}_{tr} \cap \mathcal{S}_{te} \neq \emptyset$ ,  $\mathcal{S}_{tr} \setminus \mathcal{S}_{te} \neq \emptyset$ , and  $\mathcal{S}_{te} \setminus \mathcal{S}_{tr} \neq \emptyset$ .<sup>1</sup>

The four cases are illustrated in Figure 1. We focus on cases (iii) and (iv), as they are more general and more difficult than cases (i) and (ii).

**Problem setting** Denote by  $\mathcal{X}$  and  $\mathcal{Y}$  the input and output domains, where  $\mathcal{Y} = \{1, \dots, C\}$  for  $C$ -class classification problems. Let  $\mathbf{f} : \mathcal{X} \rightarrow \mathbb{R}^C$  be a classifier (to be trained) and  $\ell : \mathbb{R}^C \times \mathcal{Y} \rightarrow (0, +\infty)$  be a loss function (for training  $\mathbf{f}$ ).<sup>2</sup> Then, the *risk* is defined as follows (Vapnik, 1998):

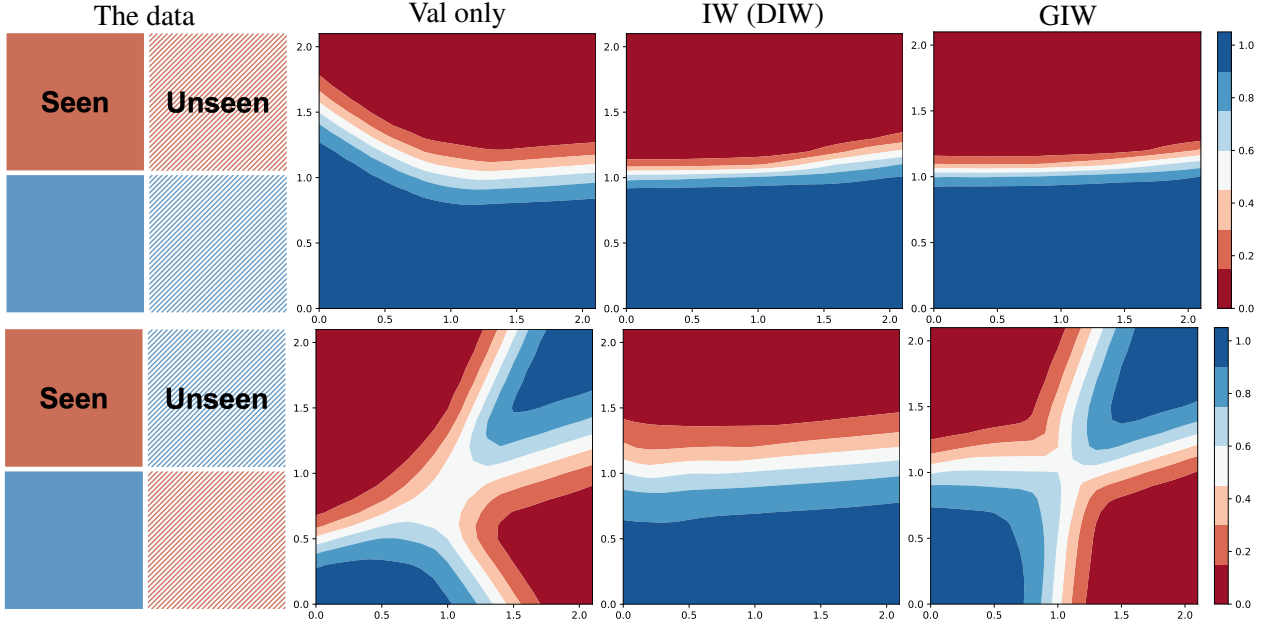
$$R(\mathbf{f}) = \mathbb{E}_{p_{te}(\mathbf{x}, y)}[\ell(\mathbf{f}(\mathbf{x}), y)], \quad (1)$$

where  $\mathbb{E}[\cdot]$  denotes the expectation. In the joint-shift problems, we are given a training set  $\mathcal{D}_{tr} = \{(\mathbf{x}_i^{tr}, y_i^{tr})\}_{i=1}^{n_{tr}} \stackrel{\text{i.i.d.}}{\sim} p_{tr}(\mathbf{x}, y)$  and a validation set  $\mathcal{D}_v = \{(\mathbf{x}_i^v, y_i^v)\}_{i=1}^{n_v} \stackrel{\text{i.i.d.}}{\sim} p_{te}(\mathbf{x}, y)$ , where  $\mathcal{D}_{tr}$  is much bigger than  $\mathcal{D}_v$ , i.e.,  $n_{tr} \gg n_v$ . The goal is to reliably estimate the risk from  $\mathcal{D}_{tr}$  and  $\mathcal{D}_v$  and train  $\mathbf{f}$  by minimizing the empirical risk, which should outperform training  $\mathbf{f}$  from only  $\mathcal{D}_v$ .

**Motivation** *Importance weighting* (IW) has been a golden solver for DS problems (Sugiyama and Kawanabe, 2012), and there are many great off-the-shelf IW methods (Huang et al., 2007; Sugiyama et al., 2007a,b; Kanamori et al., 2009). Recently, *dynamic IW* (DIW) was proposed to make IW compatible with stochastic optimizers and thus it can be used for deep learning (Fang et al., 2020). However, all IW methods including DIW have assumed cases (i) and (ii)—in cases (iii) and (iv), IW methods become ill-defined and problematic. Some IW-like methods based on bilevel optimization share a similar issue with IW (Jiang et al., 2018; Ren et al., 2018; Shu et al., 2019), since  $\mathcal{D}_v$  is used

<sup>1</sup>When  $\mathcal{S}_{tr}$  and  $\mathcal{S}_{te}$  differ, they differ by a non-zero probability measure; otherwise, we regard it as case (i). For example,  $\mathcal{S}_{te} \setminus \mathcal{S}_{tr} \neq \emptyset$  in cases (iii) and (iv) means that  $\sum_y \int_{\{\mathbf{x} : (\mathbf{x}, y) \in \mathcal{S}_{te} \setminus \mathcal{S}_{tr}\}} p_{te}(\mathbf{x}, y) d\mathbf{x} > 0$ .

<sup>2</sup>The positivity of  $\ell$ , i.e.,  $\ell(\mathbf{f}(\mathbf{x}), y) > 0$  rather than  $\ell(\mathbf{f}(\mathbf{x}), y) \geq 0$ , is needed to prove Theorem 2. This assumption holds for the popular *cross-entropy loss* and its robust variants, since  $\mathbf{f}(\mathbf{x})$  must stay finite.



This is a binary classification task for classifying blue and red colored synthetic data that are uniformly distributed in a  $2 \times 2$  grid (consists of 4 squares in different positions). Only data from the left two squares are seen by the training data and data from all squares are seen by the test/validation data. Validation data consist of one data per square of size 4. “Val only” means using only the validation data to train the model, “DIW” refers to Fang et al. (2020) and “GIW” is the proposed method. The learned decision boundary is plotted to compare the methods. In the top panel, IW and GIW perform well but in the bottom panel, IW completely fails and GIW still performs well. The performance of Val only is not satisfactory due to the limited size of validation data. More details of this experiment are presented in Section 2.

Figure 2: Two concrete examples of the success and failure of IW in case (iii).

to determine the importance weights on  $\mathcal{D}_{\text{tr}}$  and  $f$  is trained from  $\mathcal{D}_{\text{tr}}$ . In fact, cases (iii) and (iv) are more common nowadays due to *data-collection biases*, but they are still under-explored. For example, a class has several subclasses, but not all subclasses are presented in  $\mathcal{D}_{\text{tr}}$  (see Figure 2). Therefore, we want to generalize IW to a universal solver for all the four cases.

**Contributions** Our contributions can be summarized as follows.

- Firstly, we theoretically and empirically analyze when and why IW methods can succeed/may fail. We reveal that the objective of IW is good in cases (i) and (ii) and bad in cases (iii) and (iv).
- Secondly, we propose *generalized IW* (GIW). In GIW,  $\mathcal{S}_{\text{te}}$  is split into an *in-training* (IT) part  $\mathcal{S}_{\text{te}} \cap \mathcal{S}_{\text{tr}}$  and an *out-of-training* (OOT) part  $\mathcal{S}_{\text{te}} \setminus \mathcal{S}_{\text{tr}}$ , and its objective consists of a weighted classification term over the IT part and a standard classification term over the OOT part. GIW is justified as its objective is good in all the four cases and reduces to IW in cases (i) and (ii). Thus, GIW is a *strict generalization* of IW from the objective point of view.
- Thirdly, we provide a practical implementation of GIW: (a) following the split of  $\mathcal{S}_{\text{te}}$ ,  $\mathcal{D}_{\text{v}}$  is split into an IT set and an OOT set using the *one-class support vector machine* (Schölkopf et al., 1999); (b) the IT set, instead of the whole  $\mathcal{D}_{\text{v}}$ , is used for IW; and (c) the OOT set directly joins training together with  $\mathcal{D}_{\text{tr}}$  since no data in  $\mathcal{D}_{\text{tr}}$  comes from the OOT part.
- Finally, we design and conduct extensive experiments that demonstrate the effectiveness of GIW

in cases (iii) and (iv). The experiment design is also a major contribution since no experimental setup is available for reference to simulate case (iii) or (iv) on benchmark data sets.

**Organization** The analyses of IW are in Section 2, the proposal of GIW is in Section 3, and the experiments are in Section 4. Related work and additional experiments are in the appendices.

## 2 A deeper understanding of IW

First, we review the traditional *importance weighting* (IW) and its modern implementation *dynamic importance weighting* (DIW). Then, we analyze when and why IW methods can succeed/may fail.

**A review of IW** Let  $w^*(\mathbf{x}, y) = p_{\text{te}}(\mathbf{x}, y)/p_{\text{tr}}(\mathbf{x}, y)$ , which is the ratio of the test density over the training density, known as the *importance function*. Then, the *expected objective* of IW can be expressed as

$$J(\mathbf{f}) = \mathbb{E}_{p_{\text{tr}}(\mathbf{x}, y)}[w^*(\mathbf{x}, y)\ell(\mathbf{f}(\mathbf{x}), y)]. \quad (2)$$

In order to empirically approximate  $J(\mathbf{f})$  in (2), we need to have an empirical version  $\hat{w}(\mathbf{x}, y)$  of  $w^*(\mathbf{x}, y)$ , so that the *empirical objective* of IW is

$$\hat{J}(\mathbf{f}) = \frac{1}{n_{\text{tr}}} \sum_{i=1}^{n_{\text{tr}}} \hat{w}(\mathbf{x}_i^{\text{tr}}, y_i^{\text{tr}})\ell(\mathbf{f}(\mathbf{x}_i^{\text{tr}}), y_i^{\text{tr}}). \quad (3)$$

The original IW method is implemented in two steps: (I) *weight estimation* (WE) where  $\hat{w}(\mathbf{x}, y)$  is obtained and (II) *weighted classification* (WC) where  $\hat{J}(\mathbf{f})$  is minimized. The first step relies on the training data  $\mathcal{D}_{\text{tr}}$  and the validation data  $\mathcal{D}_{\text{v}}$ , and it can be either estimating the two density functions separately and taking their ratio or directly estimating the density ratio (Sugiyama et al., 2012).

**A review of DIW** DIW (Fang et al., 2020) was proposed to make IW compatible for deep learning by boosting the expressive power of the WE step in IW. Specifically, let  $\pi$  be a non-linear function to transform the data  $(\mathbf{x}, y)$  into  $\mathbf{z} = \pi(\mathbf{x}, y)$ , where  $\mathbf{z}$  can be either *loss-value* or *hidden-layer-output* representation of data created from the classifier  $\mathbf{f}$ . DIW iterates between WE and WC for computing  $\hat{w}$  on  $\mathbf{z}$  and updating  $\mathbf{f}$ . Since  $\pi$  depends on  $\mathbf{f}$ , the WE step can also enjoy deep networks and stochastic optimizers indirectly, leading to significantly improved performance on modern datasets.

**Risk consistency/inconsistency of IW** Now, consider how to qualify good or bad expected objectives under different conditions. To this end, we adopt the concepts of *risk consistency* and *classifier consistency* from the label-noise learning literature (Xia et al., 2019, 2020; Yao et al., 2020).

**Definition 1.** Given an (expected) objective  $J(\mathbf{f})$ , we say it is *risk-consistent* if  $J(\mathbf{f}) = R(\mathbf{f})$  for any  $\mathbf{f}$ , i.e., the objective is equal to the original risk for any classifier. On the other hand, we say  $J(\mathbf{f})$  is *classifier-consistent* if  $\arg \min_{\mathbf{f}} J(\mathbf{f}) = \arg \min_{\mathbf{f}} R(\mathbf{f})$  where the minimization is taken over all measurable functions, i.e., the objective shares the optimal classifier with the original risk.

Note that in the definition above, risk consistency is conceptually stronger than classifier consistency. If an objective is risk-consistent, it must also be classifier-consistent; if an objective is classifier-consistent, it may sometimes be risk-inconsistent. However, a risk-inconsistent objective is not necessarily a bad objective, as it may still be classifier-consistent. For example, if  $J(\mathbf{f}) = R(\mathbf{f})/2$  or if  $J(\mathbf{f}) = R(\mathbf{f})^2$ , minimizing  $J(\mathbf{f})$  will give the same optimal classifier as minimizing  $R(\mathbf{f})$ . Hence, when considering expected objectives, risk consistency is a sufficient condition and classifier consistency is a necessary condition for good objectives.

In what follows, we analyze when and why the objective of IW, namely  $J(\mathbf{f})$  in (2), can be a good objective or may be a bad objective.

**Theorem 1.** *In cases (i) and (ii), IW is risk-consistent.*

*Proof.* In fact, if there is only the instance random variable  $\mathbf{x}$  but no class-label random variable  $y$ , this result is simply the *importance-sampling identity* that can be found in many statistics textbooks. We prove it here to make our theoretical analyses self-contained and make later theoretical results easier to present and understand.

Recall that  $\mathcal{S}_{\text{tr}}$  is the support of  $p_{\text{tr}}(\mathbf{x}, y)$  where  $p_{\text{tr}}(\mathbf{x}, y) > 0$  and  $\mathcal{S}_{\text{te}}$  is the support of  $p_{\text{te}}(\mathbf{x}, y)$  where  $p_{\text{te}}(\mathbf{x}, y) > 0$ . Under case (i) or (ii), let us rewrite  $R(\mathbf{f})$  and  $J(\mathbf{f})$  with summations and integrals:

$$\begin{aligned} R(\mathbf{f}) &= \sum_{y=1}^C \int_{\{\mathbf{x}: (\mathbf{x}, y) \in \mathcal{S}_{\text{te}}\}} \ell(\mathbf{f}(\mathbf{x}), y) p_{\text{te}}(\mathbf{x}, y) d\mathbf{x}, \\ J(\mathbf{f}) &= \sum_{y=1}^C \int_{\{\mathbf{x}: (\mathbf{x}, y) \in \mathcal{S}_{\text{tr}}\}} \ell(\mathbf{f}(\mathbf{x}), y) w^*(\mathbf{x}, y) p_{\text{tr}}(\mathbf{x}, y) d\mathbf{x} \\ &= \sum_{y=1}^C \int_{\{\mathbf{x}: (\mathbf{x}, y) \in \mathcal{S}_{\text{tr}}\}} \ell(\mathbf{f}(\mathbf{x}), y) p_{\text{te}}(\mathbf{x}, y) d\mathbf{x}, \end{aligned}$$

where  $w^*(\mathbf{x}, y) = p_{\text{te}}(\mathbf{x}, y)/p_{\text{tr}}(\mathbf{x}, y)$  is always well-defined over  $\mathcal{S}_{\text{tr}}$  and we safely plugged this definition into the rewritten  $J(\mathbf{f})$ . Subsequently, in case (i),  $\mathcal{S}_{\text{tr}} = \mathcal{S}_{\text{te}}$  and thus  $J(\mathbf{f}) = R(\mathbf{f})$ . In case (ii),  $\mathcal{S}_{\text{tr}} \supset \mathcal{S}_{\text{te}}$  and then we further have

$$J(\mathbf{f}) = \sum_{y=1}^C \int_{\{\mathbf{x}: (\mathbf{x}, y) \in \mathcal{S}_{\text{te}}\}} \ell(\mathbf{f}(\mathbf{x}), y) p_{\text{te}}(\mathbf{x}, y) d\mathbf{x} + \int_{\{\mathbf{x}: (\mathbf{x}, y) \in \mathcal{S}_{\text{tr}} \setminus \mathcal{S}_{\text{te}}\}} \ell(\mathbf{f}(\mathbf{x}), y) p_{\text{te}}(\mathbf{x}, y) d\mathbf{x}.$$

By definition,  $p_{\text{te}}(\mathbf{x}, y) = 0$  outside  $\mathcal{S}_{\text{te}}$  including  $\mathcal{S}_{\text{tr}} \setminus \mathcal{S}_{\text{te}}$ , and thus  $J(\mathbf{f}) = R(\mathbf{f})$ .  $\square$

**Theorem 2.** *In cases (iii) and (iv), IW is risk-inconsistent, and it holds that  $J(\mathbf{f}) < R(\mathbf{f})$  for any  $\mathbf{f}$ .*

*Proof.* Since  $w^*(\mathbf{x}, y)$  is well-defined over  $\mathcal{S}_{\text{tr}}$  but it becomes ill-defined over  $\mathcal{S}_{\text{te}} \setminus \mathcal{S}_{\text{tr}}$ , we cannot naively replace the integral domain in  $J(\mathbf{f})$  as in the proof of Theorem 1. In case (iii),  $\mathcal{S}_{\text{tr}} \subset \mathcal{S}_{\text{te}}$ , and consequently

$$\begin{aligned} R(\mathbf{f}) &= \sum_{y=1}^C \int_{\{\mathbf{x}: (\mathbf{x}, y) \in \mathcal{S}_{\text{tr}}\}} \ell(\mathbf{f}(\mathbf{x}), y) p_{\text{te}}(\mathbf{x}, y) d\mathbf{x} \\ &\quad + \sum_{y=1}^C \int_{\{\mathbf{x}: (\mathbf{x}, y) \in \mathcal{S}_{\text{te}} \setminus \mathcal{S}_{\text{tr}}\}} \ell(\mathbf{f}(\mathbf{x}), y) p_{\text{te}}(\mathbf{x}, y) d\mathbf{x}. \end{aligned}$$

According to Theorem 1 for case (i), the first term in the rewritten  $R(\mathbf{f})$  equals  $J(\mathbf{f})$ . Moreover, the second term is positive, since  $\ell(\mathbf{f}(\mathbf{x}), y) > 0$  due to the positivity of  $\ell$ , and  $p_{\text{te}}(\mathbf{x}, y) > 0$  over  $\mathcal{S}_{\text{te}}$  including  $\mathcal{S}_{\text{te}} \setminus \mathcal{S}_{\text{tr}}$ . As a result, in case (iii),  $R(\mathbf{f}) > J(\mathbf{f})$ .

Similarly, in case (iv), we can split  $\mathcal{S}_{\text{te}}$  into  $\mathcal{S}_{\text{te}} \cap \mathcal{S}_{\text{tr}}$  and  $\mathcal{S}_{\text{te}} \setminus \mathcal{S}_{\text{tr}}$  and decompose  $R(\mathbf{f})$  as

$$R(\mathbf{f}) = \sum_{y=1}^C \int_{\{\mathbf{x}: (\mathbf{x}, y) \in \mathcal{S}_{\text{te}} \cap \mathcal{S}_{\text{tr}}\}} \ell(\mathbf{f}(\mathbf{x}), y) p_{\text{te}}(\mathbf{x}, y) d\mathbf{x} \\ + \sum_{y=1}^C \int_{\{\mathbf{x}: (\mathbf{x}, y) \in \mathcal{S}_{\text{te}} \setminus \mathcal{S}_{\text{tr}}\}} \ell(\mathbf{f}(\mathbf{x}), y) p_{\text{te}}(\mathbf{x}, y) d\mathbf{x}.$$

Note that  $\mathcal{S}_{\text{te}} \cap \mathcal{S}_{\text{tr}} \subset \mathcal{S}_{\text{tr}}$ , so that according to Theorem 1 for case (ii), the first term equals  $J(\mathbf{f})$ . Following case (iii), the second term is positive. Therefore, in case (iv),  $R(\mathbf{f}) > J(\mathbf{f})$ .  $\square$

Theorem 1 implies that the objective of IW can be a good objective in cases (i) and (ii). Theorem 2 implies that the objective of IW may be a bad objective in cases (iii) and (iv). For any possible implementation, as long as it honestly implements this objective, the quality of the objective will be reflected in the quality of the implementation. As a consequence, the theorems collectively address when and why IW methods can succeed/may fail.

When the IW objective may be bad and IW methods may fail, whether an IW method fails or not depends on many factors, such as the underlying data distributions, the sampled data sets, the loss, the model, and the optimizer. To illustrate this phenomenon, here we give two concrete examples belonging to case (iii), where IW has no problem at all in one example and is as poor as random guessing in the other example.

**Two concrete examples** We have seen the examples in Figure 2. In both examples, there are two classes marked with red and blue colors and distributed in four squares. Each square has a unit area and is the support of a uniform distribution of  $\mathbf{x}$ , i.e.,  $p(\mathbf{x}, 1) = 1$  and  $p(\mathbf{x}, 0) = 0$  if its color is red, and  $p(\mathbf{x}, 0) = 1$  and  $p(\mathbf{x}, 1) = 0$  if its color is blue. There is a margin of 0.1 between two adjacent squares. The training distribution consists of the two squares on the left, and the test distribution consists of all the four squares. In the first example, on  $\mathcal{S}_{\text{te}} \setminus \mathcal{S}_{\text{tr}}$ , the label is red on the top and blue on the bottom, as same as the label on  $\mathcal{S}_{\text{tr}}$ . In the second example, on  $\mathcal{S}_{\text{te}} \setminus \mathcal{S}_{\text{tr}}$ , the label is blue on the top and red on the bottom, as opposite as the label on  $\mathcal{S}_{\text{tr}}$ .

We experimentally validated whether DIW works or not. The number of training data was 200. The number of validation data was only 4: we sampled one random point from each training square and added the center point of each test-only square. We can see that DIW performs very well in the first example, better than training from only the validation data; unfortunately, DIW performs very poorly in the second example, even worse than training from only the validation data.

The observed phenomenon should not be limited to DIW but be common to all IW methods. Here, we analyze why this phenomenon does not depend on the loss, the model, or the optimizer. As the classifier  $\mathbf{f}$  can only access the information on  $\mathcal{S}_{\text{tr}}$  but must predict the class label on the whole  $\mathcal{S}_{\text{te}}$ , we assume that  $\mathbf{f}$  would transfer its knowledge about  $p_{\text{tr}}(\mathbf{x}, y)$  to  $p_{\text{te}}(\mathbf{x}, y)$  in the simplest manner. Furthermore, we simplify  $\mathbf{f}(\mathbf{x})$  into  $f(x^{(1)}, x^{(2)})$ , since it is binary classification where  $\mathbf{x} \in \mathbb{R}^2$ .

**Proposition 3.** *In the first example, IW is classifier-consistent, while in the second example, IW is classifier-inconsistent.*

*Proof.* Without loss of generality, assume that the loss  $\ell$  is *classification-calibrated* (Bartlett et al., 2006)—the popular *cross-entropy loss* is *confidence-calibrated* that is stronger than being classification-calibrated (Sugiyama et al., 2022). Let  $(c^{(1)}, c^{(2)})$  be the center of  $\mathcal{S}_{\text{te}}$ , and then the four squares are

located on the top-left, bottom-left, top-right, and bottom-right of  $(c^{(1)}, c^{(2)})$ . For convenience, we abbreviate  $f(x^{(1)}, x^{(2)})$  for  $x^{(1)} > c^{(1)}, x^{(2)} > c^{(2)}$  as  $f(+, +)$ ,  $f(x^{(1)}, x^{(2)})$  for  $x^{(1)} > c^{(1)}, x^{(2)} < c^{(2)}$  as  $f(+, -)$ , and so on.

Consider the first example. The minimizer of  $R(f)$  can be any *Bayes-optimal classifier*, i.e., any  $f$  such that  $f(\cdot, +) > 0$  and  $f(\cdot, -) < 0$ . Next, on the top-left square, we have  $p_{te}(\mathbf{x}, 1) = 1/4$ ,  $p_{te}(\mathbf{x}, 0) = 0$ ,  $p_{tr}(\mathbf{x}, 1) = 1/2$ , and  $p_{tr}(\mathbf{x}, 0) = 0$ , and thus  $w^*(\mathbf{x}, y) = 1/2$ . Likewise, on the bottom-left square, we have  $w^*(\mathbf{x}, y) = 1/2$ . As a result,  $J(f) = \frac{1}{2}\mathbb{E}_{p_{tr}(\mathbf{x}, y)}[\ell(\mathbf{f}(\mathbf{x}), y)]$ , meaning that the minimizer of  $J(f)$  can be any Bayes-optimal classifier on  $\mathcal{S}_{tr}$ , i.e., any  $f$  such that  $f(-, +) > 0$  and  $f(-, -) < 0$ . The simplest manner for  $f$  to transfer its knowledge from  $p_{tr}$  to  $p_{te}$  is to have a linear decision boundary and extend it to  $\mathcal{S}_{te} \setminus \mathcal{S}_{tr}$ , so that  $f(\cdot, +) > 0$  and  $f(\cdot, -) < 0$  on  $\mathcal{S}_{te}$ . We can see that the set of minimizers is shared and thus IW is classifier-consistent.

Consider the second example. The minimizer of  $J(f)$  is still the same while the minimizer of  $R(f)$  significantly changes to any  $f$  such that  $f(-, +) > 0$ ,  $f(-, -) < 0$ ,  $f(+, +) < 0$ , and  $f(+, -) > 0$ . This is a checkerboard where any adjacent squares have opposite signs of predictions. It is easy to see that IW is classifier-inconsistent with a test accuracy of 0.5. For binary classification with balanced classes, this accuracy is as poor as random guessing.  $\square$

### 3 Generalized importance weighting (GIW)

We have seen two examples where IW is as good/bad as possible in case (iii). In practice, we cannot rely on the luck and hope that IW would work. In this section, we propose *generalized importance weighting* (GIW), which is still IW in cases (i) and (ii) and is better than IW in cases (iii) and (iv).

#### 3.1 Expected objective of GIW

The key idea of GIW is to split the test support  $\mathcal{S}_{te}$  into the *in-training* (IT) part  $\mathcal{S}_{te} \cap \mathcal{S}_{tr}$  and the *out-of-training* (OOT) part  $\mathcal{S}_{te} \setminus \mathcal{S}_{tr}$ . More specifically, we introduce a third random variable, the support-splitting variable  $s \in \{0, 1\}$ , such that  $s$  takes 1 on  $\mathcal{S}_{tr}$  and 0 on  $\mathcal{S}_{te} \setminus \mathcal{S}_{tr}$ . As a result, the underlying joint density  $p(\mathbf{x}, y, s)$  can be defined by  $p_{te}(\mathbf{x}, y)$  as

$$p(\mathbf{x}, y, s) = \begin{cases} p_{te}(\mathbf{x}, y) & \text{if } (\mathbf{x}, y) \in \mathcal{S}_{tr} \text{ and } s = 1, \\ p_{te}(\mathbf{x}, y) & \text{if } (\mathbf{x}, y) \in \mathcal{S}_{te} \setminus \mathcal{S}_{tr} \text{ and } s = 0, \\ 0 & \text{otherwise.} \end{cases} \quad (4)$$

Here,  $p(\mathbf{x}, y, s)$  accepts  $(\mathbf{x}, y) \in \mathcal{S}_{te} \cup \mathcal{S}_{tr}$  rather than  $(\mathbf{x}, y) \in \mathcal{S}_{te}$ , and  $s$  actually splits  $\mathcal{S}_{te} \cup \mathcal{S}_{tr}$  into  $\mathcal{S}_{tr}$  and  $\mathcal{S}_{te} \setminus \mathcal{S}_{tr}$ . This is exactly the same as what we want, since  $p_{te}(\mathbf{x}, y) = 0$  outside  $\mathcal{S}_{te}$ . Let  $\alpha = p(s = 1)$ . Then, the expected objective of GIW is defined as

$$J_G(\mathbf{f}) = \alpha \mathbb{E}_{p_{tr}(\mathbf{x}, y)}[w^*(\mathbf{x}, y)\ell(\mathbf{f}(\mathbf{x}), y)] + (1 - \alpha)\mathbb{E}_{p(\mathbf{x}, y|s=0)}[\ell(\mathbf{f}(\mathbf{x}), y)]. \quad (5)$$

The corresponding empirical version  $\widehat{J}_G(\mathbf{f})$  will be derived in the next subsection. Before proceeding to the empirical objective of GIW, we establish risk consistency of GIW.

**Theorem 4.** *GIW is always risk-consistent for distribution shift problems.*

*Proof.* Let us work on the first term of  $J_G(\mathbf{f})$  in (5). When  $(\mathbf{x}, y) \in \mathcal{S}_{\text{tr}}$ ,

$$\alpha w^*(\mathbf{x}, y) p_{\text{tr}}(\mathbf{x}, y) = \alpha p_{\text{te}}(\mathbf{x}, y) = p(s=1) p(\mathbf{x}, y \mid s=1) = p(\mathbf{x}, y, s=1),$$

where  $p(\mathbf{x}, y \mid s=1) = p_{\text{te}}(\mathbf{x}, y)$  given  $(\mathbf{x}, y) \in \mathcal{S}_{\text{tr}}$  according to (4). Since  $p(\mathbf{x}, y, s=1) = 0$  on  $\mathcal{S}_{\text{te}} \setminus \mathcal{S}_{\text{tr}}$ , we have

$$\alpha \mathbb{E}_{p_{\text{tr}}(\mathbf{x}, y)} [w^*(\mathbf{x}, y) \ell(\mathbf{f}(\mathbf{x}), y)] = \sum_{y=1}^C \int_{\{\mathbf{x}: (\mathbf{x}, y) \in \mathcal{S}_{\text{te}}\}} \ell(\mathbf{f}(\mathbf{x}), y) p(\mathbf{x}, y, s=1) d\mathbf{x}. \quad (6)$$

Next, let us work on the second term of  $J_G(\mathbf{f})$  in (5). Since  $(1 - \alpha) p(\mathbf{x}, y \mid s=0) = p(\mathbf{x}, y, s=0)$ , we have

$$(1 - \alpha) \mathbb{E}_{p(\mathbf{x}, y \mid s=0)} [\ell(\mathbf{f}(\mathbf{x}), y)] = \sum_{y=1}^C \int_{\{\mathbf{x}: (\mathbf{x}, y) \in \mathcal{S}_{\text{te}}\}} \ell(\mathbf{f}(\mathbf{x}), y) p(\mathbf{x}, y, s=0) d\mathbf{x}. \quad (7)$$

Note that  $p(\mathbf{x}, y, s=1) + p(\mathbf{x}, y, s=0) = p_{\text{te}}(\mathbf{x}, y)$  according to (4). By adding (6) and (7), we can obtain that  $J_G(\mathbf{f}) = R(\mathbf{f})$ . This conclusion holds in all the four cases.  $\square$

Theorem 4 is the main theorem of this paper. It implies that the objective of GIW can always be a good objective. Recall that IW is also risk-consistent in cases (i) and (ii), and it is interesting to see how IW and GIW are connected. By definition, given fixed  $p_{\text{tr}}(\mathbf{x}, y)$  and  $p_{\text{te}}(\mathbf{x}, y)$ , if there exists a risk-consistent objective, it is unique. Indeed, in cases (i) and (ii), GIW is reduced to IW, simply due to that  $\alpha = 1$  and  $J_G(\mathbf{f}) = J(\mathbf{f})$  for any  $\mathbf{f}$ .

### 3.2 Empirical objective and practical implementation of GIW

Approximating  $J_G(\mathbf{f})$  in (5) is more involved than approximating  $J(\mathbf{f})$  in (2). Following (3), we need an empirical version  $\hat{w}(\mathbf{x}, y)$ , and we further need to split the validation data into two sets and estimate  $\alpha$ . How to accurately split the validation data  $\mathcal{D}_v$  is the most challenging part. After splitting  $\mathcal{D}_v$  and obtaining an estimate  $\hat{\alpha}$ , the empirical objective will have two terms, where the first term can be handled by any IW algorithm given training data and IT validation data, and the second term just involves OOT validation data.

To split  $\mathcal{D}_v$  and estimate  $\alpha$ , we employ the *one-class support vector machine* (O-SVM) (Schölkopf et al., 1999). Firstly, we pretrain a deep network for classification on the training data  $\mathcal{D}_{\text{tr}}$  a little bit and obtain a *feature extractor* from the pretrained deep network. Secondly, we apply the feature extractor on the instances in  $\mathcal{D}_{\text{tr}}$  and train an O-SVM based on the latent representation of these instances, giving us a score function  $g(\mathbf{z})$  that could predict whether  $p_{\text{tr}}(\mathbf{x}) > 0$  or not, where  $\mathbf{z}$  is the latent representation of  $\mathbf{x}$ . Thirdly, we apply the feature extractor on the instances in  $\mathcal{D}_v$  and then employ  $g(\mathbf{z})$  to obtain the IT validation data  $\mathcal{D}_{v1} = \{(\mathbf{x}_i^{v1}, y_i^{v1})\}_{i=1}^{n_{v1}}$  and the OOT validation data  $\mathcal{D}_{v2} = \{(\mathbf{x}_i^{v2}, y_i^{v2})\}_{i=1}^{n_{v2}}$ . Finally,  $\alpha$  can be naturally estimated as  $\hat{\alpha} = n_{v1}/n_v$ .

We have two comments on the split of  $\mathcal{D}_v$ . The O-SVM  $g(\mathbf{z})$  predicts whether  $p_{\text{tr}}(\mathbf{x}) > 0$  or not rather than whether  $p_{\text{tr}}(\mathbf{x}, y) > 0$  or not. This is because the  $\mathbf{x}$ -support change is often sufficiently informative in practice: when the  $\mathbf{x}$ -support changes, O-SVM can detect it; the  $(\mathbf{x}, y)$ -support change without any  $\mathbf{x}$ -support change rarely happens, and when it happens, it is very difficult to train an



---

**Algorithm 1** Generalized importance weighting (GIW).
 

---

<b>Input:</b> initial model $\mathbf{f}_\theta$ parameterized by $\theta$ training data $\mathcal{D}_{\text{tr}}$ validation data $\mathcal{D}_{\text{v}}$ batch size $m, n_1, n_2$ max iteration $T$	<b>procedure 2.</b> MODELUPDATE( $\mathcal{D}_{\text{tr}}, \mathcal{D}_{\text{v1}}, \mathcal{D}_{\text{v2}}, \hat{\alpha}$ ) 1: <b>for</b> $t = 1$ to $T$ <b>do</b> 2: $\mathcal{S}_{\text{tr}} \leftarrow \text{SampleMiniBatch}(\mathcal{D}_{\text{tr}}, m)$ 3: $\mathcal{S}_{\text{v1}} \leftarrow \text{SampleMiniBatch}(\mathcal{D}_{\text{v1}}, n_1)$ 4: $\mathcal{S}_{\text{v2}} \leftarrow \text{SampleMiniBatch}(\mathcal{D}_{\text{v2}}, n_2)$ 5:     forward $\mathcal{S}_{\text{tr}}$ & $\mathcal{S}_{\text{v1}}$ 6:     compute loss values as $\mathcal{L}_{\text{tr}}$ & $\mathcal{L}_{\text{v1}}$ 7:     match $\mathcal{L}_{\text{tr}}$ & $\mathcal{L}_{\text{v1}}$ to obtain $\mathcal{W}$ by DIW 8:     weight loss on $\mathcal{S}_{\text{tr}}$ by $\mathcal{W}$ 9:     forward $\mathcal{S}_{\text{v2}}$ 10:     compute loss on $\mathcal{S}_{\text{v2}}$ 11:     backward $\hat{J}_{\text{G}}(\mathbf{f}_{\theta_t})$ and update $\theta_t$ by (8) 12: <b>end for</b> 13: <b>return</b> $\mathbf{f}_{\theta_T}$ 14: <b>end procedure</b>
1: <b>procedure 1.</b> VALDATASPLIT( $\mathcal{D}_{\text{tr}}, \mathcal{D}_{\text{v}}$ ) 2:     pretrain the model on $\mathcal{D}_{\text{tr}}$ as $\mathbf{f}_{\theta_0}$ 3:     forward input parts of $\mathcal{D}_{\text{tr}}$ & $\mathcal{D}_{\text{v}}$ 4:     retrieve transformed $\mathcal{Z}_{\text{tr}}$ & $\mathcal{Z}_{\text{v}}$ 5:     train an O-SVM on $\mathcal{Z}_{\text{tr}}$ 6:     compute O-SVM scores for $\mathcal{Z}_{\text{v}}$ 7:     partition $\mathcal{D}_{\text{v}}$ into $\mathcal{D}_{\text{v1}}$ & $\mathcal{D}_{\text{v2}}$ 8:     estimate $\hat{\alpha} =  \mathcal{D}_{\text{v1}} / \mathcal{D}_{\text{v}} $ 9: <b>return</b> $\mathcal{D}_{\text{v1}}, \mathcal{D}_{\text{v2}}, \hat{\alpha}$ 10: <b>end procedure</b>	

---

O-SVM based on the loss value instead of the latent representation to detect the change. The other comment is about the choice of the O-SVM. While there are more advanced one-class classification methods (Hido et al., 2011; Zaheer et al., 2020; Hu et al., 2020; Goldwasser et al., 2020) (see Perera et al. (2021) for a survey), the O-SVM is already good enough for the purpose (see Appendix C.1).

Subsequently,  $\mathcal{D}_{\text{v1}}$  can be viewed as being drawn from  $p(\mathbf{x}, y \mid s = 1)$ , and  $\mathcal{D}_{\text{v2}}$  can be viewed as being drawn from  $p(\mathbf{x}, y \mid s = 0)$ . Based on  $\mathcal{D}_{\text{tr}}$  and  $\mathcal{D}_{\text{v1}}$ , we can obtain either  $\hat{w}(\mathbf{x}, y)$  or  $\hat{w}_i$  for each  $(\mathbf{x}_i^{\text{tr}}, y_i^{\text{tr}})$  by IW. IW has no problem here since the split of  $\mathcal{D}_{\text{v}}$  can reduce case (iii) to case (i) and case (iv) to case (ii). In the implementation, we employ DIW (Fang et al., 2020) because it is friendly to deep learning and it is a state-of-the-art IW method. Finally, the empirical objective of GIW can be expressed as

$$\hat{J}_{\text{G}}(\mathbf{f}) = \frac{n_{\text{v1}}}{n_{\text{v}}n_{\text{tr}}} \sum_{i=1}^{n_{\text{tr}}} \hat{w}(\mathbf{x}_i^{\text{tr}}, y_i^{\text{tr}}) \ell(\mathbf{f}(\mathbf{x}_i^{\text{tr}}), y_i^{\text{tr}}) + \frac{1}{n_{\text{v}}} \sum_{j=1}^{n_{\text{v2}}} \ell(\mathbf{f}(\mathbf{x}_j^{\text{v2}}), y_j^{\text{v2}}), \quad (8)$$

where the two expectations in  $J_{\text{G}}(\mathbf{f})$  are approximated separately with  $\mathcal{D}_{\text{tr}}$  and  $\mathcal{D}_{\text{v2}}$ .<sup>3</sup>

The GIW algorithm is presented in Algorithm 1, where  $\mathcal{Z}$  denotes the hidden-layer-output (-F) representation of data. In procedure 2, we adopt the loss-value (-L) representation of data to estimate  $w$  in every mini-batch; -F representation is also tried as an ablation study in Section 4.3. As updating the model,  $\hat{w}$  also changes dynamically due to the changes in the -F/-L representation of data.

---

<sup>3</sup>In GIW, although  $J_{\text{G}}(\mathbf{f}) = R(\mathbf{f})$ ,  $\hat{J}_{\text{G}}(\mathbf{f})$  is not an unbiased estimator of  $J_{\text{G}}(\mathbf{f})$ . This is exactly the same as what in IW, where  $\hat{J}(\mathbf{f})$  is not an unbiased estimator of  $J(\mathbf{f})$  when  $J(\mathbf{f}) = R(\mathbf{f})$ . It is mainly due to that  $\hat{w}(\mathbf{x}, y)$  is not unbiased to  $w^*(\mathbf{x}, y)$ . Nevertheless, for advanced IW methods such as Kanamori et al. (2009),  $\hat{w}(\mathbf{x}, y)$  can be statistically consistent with  $w^*(\mathbf{x}, y)$ , i.e.,  $\hat{w}(\mathbf{x}, y) \rightarrow w^*(\mathbf{x}, y)$  almost surely as  $n_{\text{tr}}, n_{\text{v}} \rightarrow \infty$ . If so, we can establish statistical consistency of  $\hat{J}_{\text{G}}(\mathbf{f})$  with  $J_{\text{G}}(\mathbf{f})$  for any  $\mathbf{f}$ . If we further assume that the function class of  $\mathbf{f}$  has a bounded complexity and  $\ell$  is bounded and Lipschitz continuous, we can establish statistical consistency of  $R(\hat{\mathbf{f}})$  with  $R(\mathbf{f}^*)$ , where  $\hat{\mathbf{f}}(\mathbf{x})$  and  $\mathbf{f}^*(\mathbf{x})$  are the minimizers of  $\hat{J}_{\text{G}}(\mathbf{f})$  and  $R(\mathbf{f})$ .

Since  $n_v \ll n_{tr}$ , when using stochastic batched optimization, it may be difficult to use the same proportionate amount of training/validation data relative to its whole in every mini-batch for ensuring that they go through only once per epoch. So we define an epoch as the single loop over the training data and increase the sampling frequency of validation data by passing it multiple times per epoch.

## 4 Experiments

In this section, we present empirical evaluations of GIW and baselines. We first show experimental results on benchmark datasets with only the support shift. Then we consider the cases of support-distribution shift, i.e., adding label noise or class-prior shift on top of the support shift. Finally, we conduct ablation studies with different sample sizes and choices of data representation. Details of experimental setups and more results can be found in Appendix B and C.

To analyze GIW, we compare it with the following baseline methods:

- *Val only* uses only the validation data to train the model from scratch;
- *Pretrain val* uses the validation data to train the model after pretrained on the training data;
- *Reweight* learns to reweight data by minimizing the validation loss (Ren et al., 2018);
- *MW-Net*, short for *Meta-Weight-Net*, uses an MLP to learn a weighting function (Shu et al., 2019);
- *R-DIW* is *relative unconstrained least-squares importance fitting* (Yamada et al., 2011), where  $\alpha$ -relative density-ratio is estimated as weight, being modified in DIW fashion to use deep learning;
- *DIW* is the *dynamic importance weighting* method (Fang et al., 2020).

### 4.1 Support shift

Here we present the setups for experiments under support shift on benchmark datasets, shown in Table 1. For MNIST, we classify odd and even digits where the training data contain only 4 digits (0-3), and the test data contain 10 digits (0-9) in case (iii) and 8 digits (2-9) in case (iv). We sample 2 data per test data digit as the validation data of size 20 in case (iii) and size 16 in case (iv). Color-MNIST is modified from MNIST for 10-digit classification where the digits in training data are colored in red while in test/validation data are colored in red/blue/green evenly. We sample 2 data per digit as the validation data of size 20. CIFAR-100 has 100 classes that are defined within 20 superclasses. We call it CIFAR-20 when using it for 20-superclass classification, where the training set contain only data from 2 out of the 5 classes in each superclass while the test set contain all

Table 1: Specification of benchmark datasets, tasks, setups, and models.

Dataset	Task (classification for)	Training data	Test data	Model
MNIST	odd and even digits	4 digits (0-3)	10 digits (0-9)*	LeNet-5
Color-MNIST	10 digits	digits all in red	digits in red/blue/green	LeNet-5
CIFAR-20	objects in 20 superclasses	2 classes/superclass	5 classes/superclass	ResNet-18

See <http://yann.lecun.com/exdb/mnist/> for MNIST and Color-MNIST (LeCun et al., 1998), and <https://www.cs.toronto.edu/~kriz/cifar.html> for CIFAR-20 (Krizhevsky and Hinton, 2009). Models are modified LeNet-5 (LeCun et al., 1998) (see Appendix B.1 for details) and ResNet-18 (He et al., 2016). \* All setups in the table are in case (iii); in case (iv) on MNIST, test data consist of 8 digits (2-9).

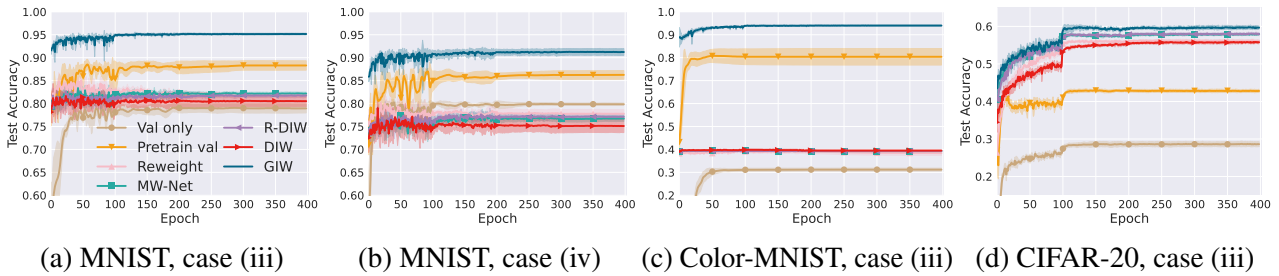


Figure 3: Results on MNIST, Color-MNIST, and CIFAR-20 under support shift (5 trails).

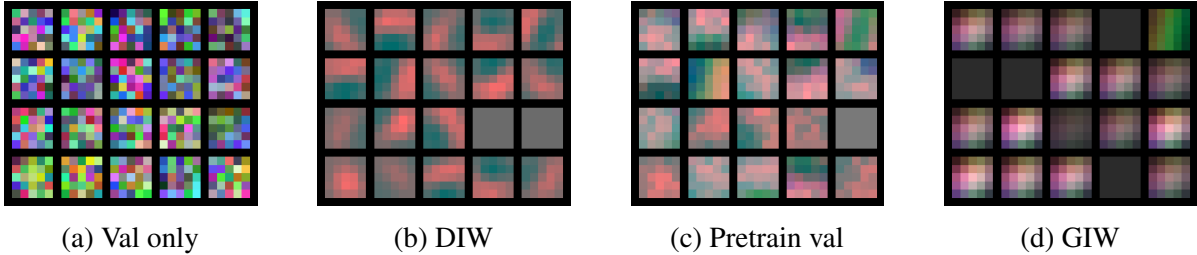


Figure 4: Visualizations of the learned convolution kernels on Color-MNIST under support shift.

classes. We sample 10 data per class as the validation data of size 1000.

Figure 3 shows the results on MNIST, Color-MNIST, and CIFAR-20 under support shift, where GIW outperforms other methods. We also confirm that  $\alpha$  in (5) is estimated correctly, as shown in Appendix C.1. For the Color-MNIST experiments, we further visualize the learned weights/kernels in convolutional layers in Figure 4, where the intensity of one color represents the weights learned on that colored channel. We find that DIW learns weights only on the red channel and Pretrain val learns weights mainly on the red channel, which may make them fail on the test data with green/blue color. Val only has weights on all channels but may fail to learn useful representations. GIW recovers the weights of all colored channels and generalizes the best to the test data.

## 4.2 Support-distribution shift

We further impose distribution shift, i.e., adding label noise or class-prior shift, on top of the support shift following the same setup in Table 1. Here we only show the results in case (iii) and put the results in case (iv) to Appendix C.3 due to the space limitation.

**Label-noise experiments** In addition to the support shift, we impose label noise by randomly flipping a label to other classes with an equal probability, i.e., the noise rate. The noise rates are set as  $\{0.2, 0.4\}$  and the corresponding experimental results are shown in Figure 5. We can see that compared with baselines, GIW performs better and tends to be robust to noisy labels.

**Class-prior-shift experiments** On top of the support shift, we impose class-prior shift by reducing the number of training data in half of the classes to make them minority classes (as opposed to

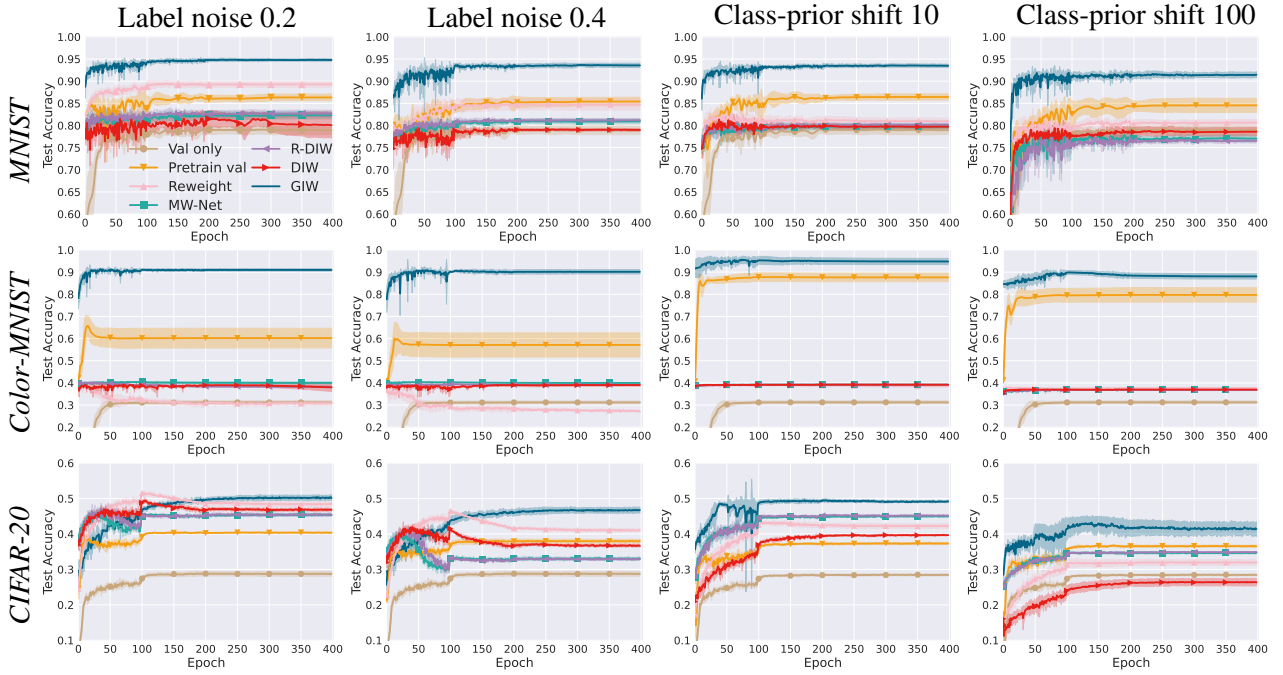
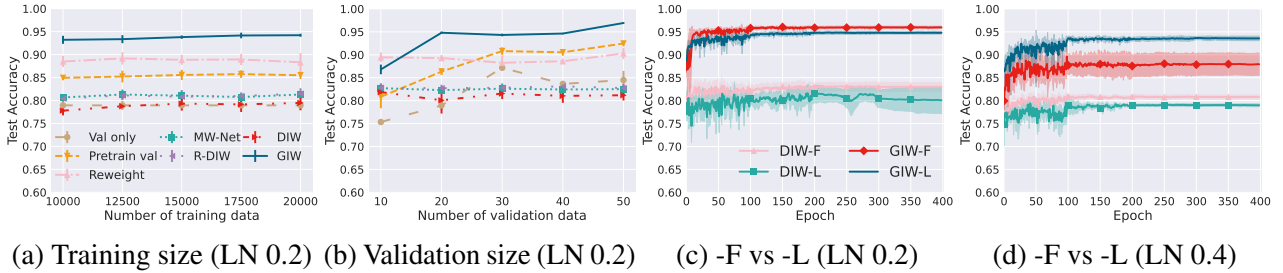


Figure 5: Results on MNIST, Color-MNIST, and CIFAR-20 under support-distribution shift (5 trails).



(a) Training size (LN 0.2) (b) Validation size (LN 0.2) (c) -F vs -L (LN 0.2) (d) -F vs -L (LN 0.4)

Figure 6: Results on using different sample sizes and data representations. LN stands for label noise.

majority classes). The sample size ratio per class between the majority and minority classes is defined as  $\rho$ , chosen from  $\{10, 100\}$ . To fully use the data from the minority class, we do not split the validation data in class-prior-shift experiments and use all validation data in optimizing the two terms in (8). From the results in Figure 5, we can see that GIW performs better than the baselines.

### 4.3 Ablation study

Finally, we study the effect of using different sample sizes and data representations on MNIST under label noise. In Figure 6a, the performance of all methods is nearly unchanged with varying  $n_{tr}$ ; in Figure 6b, GIW performs better with more validation data, e.g., when  $n_v$  increases from 10 to 20. Furthermore, we compare the loss-value (-L) with the hidden-layer-output (-F) representation of data used in the methods. Figure 6c, 6d show that -F and -L methods perform similarly under

0.2 label-noise experiments, but GIW-F is worse than GIW-L under 0.4 label noise. Therefore, we suggest using the GIW-L method, especially for situations under severe label noise.

## 5 Conclusions

We analyzed the success and failure of IW and generalized IW to allow a wider test support. Specifically, we found that in cases (i) and (ii), IW is risk-consistent, while in cases (iii) and (iv), the IW risk consistency no longer holds, and a weaker notion of it, the classifier consistency of IW, only holds sometimes. Then we proposed GIW as a universal solver that is risk-consistent in all the four cases. Experiments on various settings in cases (iii) and (iv) demonstrated the effectiveness of GIW. Potential limitations are twofold: ensuring the distributions of validation and test data to be precisely the same may be difficult in practice. Using the limited OOT validation data in both training and validation may lead to an over-optimistic expectation of the test performance.

## References

- P. L. Bartlett, M. I. Jordan, and J. D. McAuliffe. Convexity, classification, and risk bounds. *Journal of the American Statistical Association*, 101(473):138–156, 2006.
- S. Ben-David, J. Blitzer, K. Crammer, and F. Pereira. Analysis of representations for domain adaptation. In *NeurIPS*, 2006.
- J. Duchi, P. Glynn, and H. Namkoong. Statistics of robust optimization: A generalized empirical likelihood approach. *arXiv preprint arXiv:1610.03425*, 2016.
- T. Fang, N. Lu, G. Niu, and M. Sugiyama. Rethinking importance weighting for deep learning under distribution shift. In *NeurIPS*, 2020.
- Y. Ganin, E. Ustinova, H. Ajakan, P. Germain, H. Larochelle, F. Laviolette, M. March, and V. Lempitsky. Domain-adversarial training of neural networks. *Journal of Machine Learning Research*, 17(59):1–35, 2016.
- S. Goldwasser, A. T. Kalai, Y. Kalai, and O. Montasser. Beyond perturbations: Learning guarantees with arbitrary adversarial test examples. In *NeurIPS*, 2020.
- M. Gong, K. Zhang, T. Liu, D. Tao, C. Glymour, and B. Schölkopf. Domain adaptation with conditional transferable components. In *ICML*, 2016.
- I. Goodfellow, Y. Bengio, and A. Courville. *Deep learning*. The MIT Press, 2016.
- K. He, X. Zhang, S. Ren, and J. Sun. Deep residual learning for image recognition. In *CVPR*, 2016.
- S. Hido, Y. Tsuboi, H. Kashima, M. Sugiyama, and T. Kanamori. Statistical outlier detection using direct density ratio estimation. *Knowledge and information systems*, 26:309–336, 2011.
- W. Hu, M. Wang, Q. Qin, J. Ma, and B. Liu. Hrn: A holistic approach to one class learning. In *NeurIPS*, 2020.

- J. Huang, A. Gretton, K. Borgwardt, B. Schölkopf, and A. Smola. Correcting sample selection bias by unlabeled data. In *NeurIPS*, 2007.
- S. Ioffe and C. Szegedy. Batch normalization: Accelerating deep network training by reducing internal covariate shift. In *ICML*, 2015.
- L. Jiang, Z. Zhou, T. Leung, L.-J. Li, and L. Fei-Fei. Mentornet: Learning data-driven curriculum for very deep neural networks on corrupted labels. In *ICML*, 2018.
- T. Kanamori, S. Hido, and M. Sugiyama. A least-squares approach to direct importance estimation. *Journal of Machine Learning Research*, 10(7):1391–1445, 2009.
- D. P. Kingma and J. L. Ba. Adam: A method for stochastic optimization. In *ICLR*, 2015.
- A. Krizhevsky and G. Hinton. Learning multiple layers of features from tiny images. Technical report, Citeseer, 2009.
- Y. LeCun, L. Bottou, Y. Bengio, and P. Haffner. Gradient-based learning applied to document recognition. *Proceedings of the IEEE*, 86(11):2278–2324, 1998.
- S. Pan and Q. Yang. A survey on transfer learning. *IEEE Transactions on Knowledge and Data Engineering*, 22(10):1345–1359, 2009.
- P. Perera, P. Oza, and V. M. Patel. One-class classification: A survey. *arXiv preprint arXiv:2101.03064*, 2021.
- J. Quionero-Candela, M. Sugiyama, A. Schwaighofer, and N. Lawrence. *Dataset shift in machine learning*. The MIT Press, 2009.
- M. Ren, W. Zeng, B. Yang, and R. Urtasun. Learning to reweight examples for robust deep learning. In *ICML*, 2018.
- K. Saito, Y. Ushiku, and T. Harada. Asymmetric tri-training for unsupervised domain adaptation. In *ICML*, 2017.
- B. Schölkopf, R. C. Williamson, A. Smola, J. Shawe-Taylor, and J. Platt. Support vector method for novelty detection. In *NeurIPS*, 1999.
- J. Shu, Q. Xie, L. Yi, Q. Zhao, S. Zhou, Z. Xu, and D. Meng. Meta-weight-net: Learning an explicit mapping for sample weighting. In *NeurIPS*, 2019.
- M. Sugiyama and M. Kawanabe. *Machine learning in non-stationary environments: Introduction to covariate shift adaptation*. The MIT Press, 2012.
- M. Sugiyama, M. Krauledat, and K. Müller. Covariate shift adaptation by importance weighted cross validation. *Journal of Machine Learning Research*, 8(5):985–1005, 2007a.
- M. Sugiyama, S. Nakajima, H. Kashima, P. Buenau, and M. Kawanabe. Direct importance estimation with model selection and its application to covariate shift adaptation. In *NeurIPS*, 2007b.
- M. Sugiyama, T. Suzuki, and T. Kanamori. *Density ratio estimation in machine learning*. Cambridge University Press, 2012.

- M. Sugiyama, H. Bao, T. Ishida, N. Lu, T. Sakai, and G. Niu. *Machine learning from weak supervision: An empirical risk minimization approach*. The MIT Press, 2022.
- V. N. Vapnik. *Statistical learning theory*. John Wiley & Sons, 1998.
- X. Xia, T. Liu, N. Wang, B. Han, C. Gong, G. Niu, and M. Sugiyama. Are anchor points really indispensable in label-noise learning? In *NeurIPS*, 2019.
- X. Xia, T. Liu, B. Han, N. Wang, M. Gong, H. Liu, G. Niu, D. Tao, and M. Sugiyama. Part-dependent label noise: Towards instance-dependent label noise. In *NeurIPS*, 2020.
- M. Yamada, T. Suzuki, T. Kanamori, H. Hachiya, and M. Sugiyama. Relative density-ratio estimation for robust distribution comparison. In *NeurIPS*, 2011.
- Y. Yao, T. Liu, B. Han, M. Gong, J. Deng, G. Niu, and M. Sugiyama. Dual T: Reducing estimation error for transition matrix in label-noise learning. In *NeurIPS*, 2020.
- M. Z. Zaheer, J.-h. Lee, M. Astrid, and S.-I. Lee. Old is gold: Redefining the adversarially learned one-class classifier training paradigm. In *CVPR*, 2020.

# Supplementary Material

## A Related work

In this section, we discuss relevant prior studies for addressing distribution shift problems, including importance weighting (IW), IW-like methods, and domain adaptation (DA).

**Importance weighting (IW)** IW has been a powerful tool for mitigating the influence of distribution shifts. The general idea is first to estimate the importance, which is the test over training density ratio, and then train a classifier by weighting the training losses according to the importance. Numerous IW methods have been developed in this manner, utilizing different techniques for importance estimation.

The *kernel mean matching* (KMM) approach (Huang et al., 2007) learns the importance function by matching the distributions of training and test data in terms of the maximum mean discrepancy in a reproducing kernel Hilbert space, while the *Kullback-Leibler importance estimation procedure* (KLIEP) (Sugiyama et al., 2007b) employs the KL divergence for density fitting and the *least-squares importance fitting* (LSIF) (Kanamori et al., 2009) employs squared loss for importance fitting. The *unconstrained LSIF* (uLSIF) (Kanamori et al., 2009) is an approximation version of LSIF that removes the non-negativity constraint in optimization, allowing for more efficient computation. To boost the performance of such traditional IW methods, *dynamic importance weighting* (DIW) (Fang et al., 2020) is recently proposed to make them compatible with stochastic optimizers, thereby facilitating their effective integration with deep learning frameworks.

However, in order to establish a well-defined notion of importance, all IW methods including DIW assume cases (i) and (ii), while they become problematic in cases (iii) and (iv).

**IW-like methods** A notable IW invariant is the *relative unconstrained least-squares importance fitting* (RuLSIF) (Yamada et al., 2011), which considers a smoothed and bounded extension of the importance. Instead of estimating the importance  $w^*(\mathbf{x}, y) = p_{\text{te}}(\mathbf{x}, y)/p_{\text{tr}}(\mathbf{x}, y)$ , they estimate the  $\eta$ -relative importance  $w_\eta^*(\mathbf{x}, y) = p_{\text{te}}(\mathbf{x}, y) / (\eta p_{\text{te}}(\mathbf{x}, y) + (1 - \eta)p_{\text{tr}}(\mathbf{x}, y))$  where  $0 \leq \eta \leq 1$ . While the relative importance is well-defined in cases (iii) and (iv), experiments have demonstrated that it is inferior to GIW, primarily because its training does not incorporate any data from the out-of-training (OOT) part.

Moreover, some reweighting approaches based on bilevel optimization look like DIW in the sense of iterative training between weighted classification on the training data for learning the classifier and weight estimation with the help of a small set of validation data for learning the weights (Jiang et al., 2018; Ren et al., 2018; Shu et al., 2019). However, they encounter similar issues as IW and RuLSIF, where validation data is solely used for learning the weights, while the training data (without any OOT data) is used for training the classifier.

**Domain adaptation (DA)** DA relates to DS problems where the  $p_{\text{te}}(\mathbf{x}, y)$  and  $p_{\text{tr}}(\mathbf{x}, y)$  are usually named as target and source domain distributions (Ben-David et al., 2006), or in-domain and out-of-domain distributions (Duchi et al., 2016). It can be categorized into *supervised* DA (SDA) or



*unsupervised* DA (UDA): the former has labeled test data while the latter has unlabeled test data. SDA has a similar setting as GIW, while UDA is more popular in DA. Based on different assumptions, UDA involves learning domain-invariant (Ganin et al., 2016) or conditional domain-invariant features (Gong et al., 2016), or giving pseudo labels to the target domain data (Saito et al., 2017).

## B Supplementary information on experimental setup

In this section, we present supplementary information on the experimental setup. All experiments were implemented using PyTorch 1.13.1<sup>4</sup> and carried out on NVIDIA Tesla V100 GPUs<sup>5</sup>.

### B.1 Datasets and base models

**MNIST** MNIST (LeCun et al., 1998) is a 28\*28 grayscale image dataset for 10 hand-written digits (0–9). The original dataset includes 60,000 training data and 10,000 test data. See <http://yann.lecun.com/exdb/mnist/> for more details.

In the experiments, we converted it for binary classification to classify even/odd digits as follows:

- Class 0: digits ‘0’, ‘2’, ‘4’, ‘6’, and ‘8’;
- Class 1: digits ‘1’, ‘3’, ‘5’, ‘7’, and ‘9’.

In our setup, the training data only included 4 digits (0-4). The test data could access all digits (0-9) in case (iii) and 8 digits (2-9) in case (iv). Since the number of training data was reduced, we added two data augmentations to the training and validation data: random rotation with degree 10 and random affine transformation with degree 10, translate of (0.1, 0.1) and scale of (0.9, 1.1). Note that the data augmentation was only added in procedure 2 of Algorithm 1.

Accordingly, we modified LeNet-5 (LeCun et al., 1998) as the base model for MNIST:

- 0th (input) layer: (32\*32)-
- 1st layer: C(5\*5,6)-S(2\*2)-
- 2nd layer: C(5\*5,16)-S(2\*2)-
- 3rd layer: FC(120)-
- 4th to 5th layer: FC(84)-2,

where C(5\*5,6) represents a 5\*5 convolutional layer with 6 output channels followed by ReLU, S(2\*2) represents a max-pooling layer with a filter of size 2\*2, and FC(120) represents a fully connected layer with 120 outputs followed by ReLU, etc. The hidden-layer-output representation of data used in the implementation was the normalized output extracted from the 3rd layer.

**Color-MNIST** Color-MNIST was modified from MNIST for 10 hand-written digit classification, where the digits in training data were colored in red and the digits in test/validation data were colored in either red, green or blue evenly. See Figure 7 for illustrations of the training and validation data. We did not add any data augmentation for experiments on Color-MNIST.

---

<sup>4</sup><https://pytorch.org>

<sup>5</sup><https://www.nvidia.com/en-us/data-center/v100/>

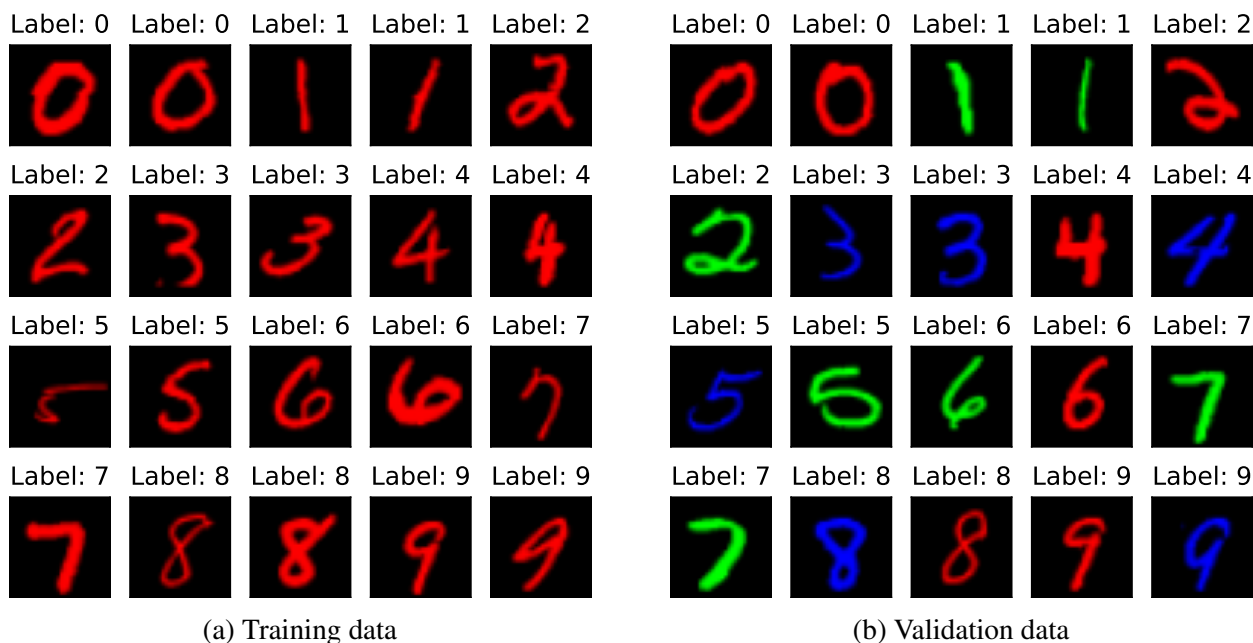


Figure 7: Illustrations of the training and validation data in Color-MNIST dataset.

To process RGB input data, we modified LeNet-5 as the base model for Color-MNIST:

- 0th (input) layer:  $(32*32*3)$ -
- 1st layer:  $C(5*5,20)$ - $S(2*2)$ -
- 2nd layer:  $C(5*5,50)$ - $S(2*2)$ -
- 3rd layer:  $FC(120)$ -
- 4th to 5th layer:  $FC(84)$ -10,

where the abbreviations and the way of extracting the hidden-layer-output representation of data were the same as that in MNIST.

**CIFAR-20** CIFAR-100 (Krizhevsky and Hinton, 2009) is a  $32*32$  colored image dataset in 100 classes, grouped in 20 superclasses. It contains 50,000 training data and 10,000 test data. We call this dataset CIFAR-20 when using it for 20-superclass classification—the pre-defined superclasses and classes as shown below, where each superclass includes five distinct classes. See <https://www.cs.toronto.edu/~kriz/cifar.html> for more details.

In our setup, the training data only included the data in 2 out of 5 classes per superclass, i.e., the classes in ( ) were seen by the training data as shown below. The test data included the data in all classes. Since the number of training data was reduced, we added several data augmentations to the training and validation data: random horizontal flip, random vertical flip, random rotation of degree 10 and random crop of size 32 with padding 4. Note that the data augmentation was only added in procedure 2 of Algorithm 1.

Superclass	Class
aquatic mammals	(beaver, dolphin), otter, seal, whale
fish	(aquarium fish, flatfish), ray, shark, trout
flowers	(orchids, poppies), roses, sunflowers, tulips
food containers	(bottles, bowls), cans, cups, plates
fruit and vegetables	(apples, mushrooms), oranges, pears, sweet peppers
household electrical devices	(clock, computer keyboard), lamp, telephone, television
household furniture	(bed, chair), couch, table, wardrobe
insects	(bee, beetle), butterfly, caterpillar, cockroach
large carnivores	(bear, leopard), lion, tiger, wolf
large man-made outdoor things	(bridge, castle), house, road, skyscraper
large natural outdoor scenes	(cloud, forest), mountain, plain, sea
large omnivores and herbivores	(camel, cattle), chimpanzee, elephant, kangaroo
medium-sized mammals	(fox, porcupine), possum, raccoon, skunk
non-insect invertebrates	(crab, lobster), snail, spider, worm
people	(baby, boy), girl, man, woman
reptiles	(crocodile, dinosaur), lizard, snake, turtle
small mammals	(hamster, mouse), rabbit, shrew, squirrel
trees	(maple, oak), palm, pine, willow
vehicles 1	(bicycle, bus), motorcycle, pickup truck, train
vehicles 2	(lawn-mower, rocket), streetcar, tank, tractor

As for the base model for CIFAR-20, we adopted ResNet-18 (He et al., 2016) as follows:

0th (input) layer: (32\*32\*3)-

1st to 5th layers: C(3\*3, 64)-[C(3\*3, 64), C(3\*3, 64)]\*2-

6th to 9th layers: [C(3\*3, 128), C(3\*3, 128)]\*2-

10th to 13th layers: [C(3\*3, 256), C(3\*3, 256)]\*2-

14th to 17th layers: [C(3\*3, 512), C(3\*3, 512)]\*2-

18th layer: Global Average Pooling-20,

where [ ·, · ] denotes a building block (He et al., 2016) and [·]\*2 means 2 such blocks, etc. Batch normalization (Ioffe and Szegedy, 2015) was applied after convolutional layers. The hidden-layer-output representation of data was the normalized output after pooling operation in the 18th layer.

## B.2 Experiments under support shift

For all compared methods except Val only, we pre-trained the model for 10 epochs as the initialization. For the one-class support vector machine (O-SVM) (Schölkopf et al., 1999), we adopted the implementation from scikit-learn<sup>6</sup>, where the radial basis function (RBF) kernel was used:  $k(\mathbf{x}_i, \mathbf{x}_j) = e^{-\gamma\|\mathbf{x}_i - \mathbf{x}_j\|^2}$  with  $\gamma = 10000$ . All other hyperparameters about O-SVM were set as the default. For the distribution matching by dynamic importance weighting (DIW) (Fang et al., 2020),

<sup>6</sup><https://scikit-learn.org/stable/modules/generated/sklearn.svm.OneClassSVM.html>

we again used the RBF kernel where  $\gamma$  was the median distance of the training data. And we used  $\mathbf{K} + \omega \mathbf{I}$  as the kernel matrix  $\mathbf{K}$ , where  $\mathbf{I}$  was an identity matrix and  $\omega$  was set to be  $1e-05$ . The upper bound of weights was set as 50.

In all experiments under support shift, Adam (Kingma and Ba, 2015) was used as the optimizer, the learning rate was 0.0005, decaying every 100 epochs by multiplying a factor of 0.1, and the batch size was set as 256. For MNIST, Color-MNIST, and CIFAR-20 experiments, the weight decay was set as 0.005, 0.002, and 0.0001, respectively.

### B.3 Experiments under support-distribution shift

For experiments under support-distribution shift, all the setups and hyperparameters about the initialization, O-SVM, and distribution matching by DIW were the same as that in Section B.2. Moreover, the same that Adam was used as the optimizer, the learning rate was 0.0005, decaying every 100 epochs by multiplying a factor of 0.1, and the batch size was set as 256. Next we show the setups and hyperparameters specific to the support-distribution shift.

**Label-noise experiments** On top of the support shift in Section B.2, we added a symmetric label noise to the training data, where a label may flip to all other classes with an equal probability (this probability was defined as the noise rate, set as  $\{0.2, 0.4\}$ ). The type of label noise and the noise rate were unknown to the model. For MNIST, Color-MNIST, and CIFAR-20 experiments, the weight decay was set as 0.005, 0.002, and  $5e-05$ , respectively.

**Class-prior shift experiments** We induced class-prior shift in the training data by randomly sampling half of the classes as minority classes (other classes were the majority classes) and reducing the number of samples in minority classes. The sample size ratio per class between the majority and minority classes was  $\rho$ , chosen from  $\{10, 100\}$ . The selected minority classes in class-prior shift experiments were:

- MNIST: class of odd digits;
- Color-MNIST: digits ‘1’, ‘2’, ‘6’, ‘7’, and ‘8’;
- CIFAR-20: superclasses of ‘fish’, ‘fruit and vegetables’, ‘household electrical device’, ‘household furniture’, ‘large carnivores’, ‘large omnivores and herbivores’, ‘medium-sized mammals’, ‘people’, ‘small mammals’, and ‘vehicles 1’.

For MNIST, Color-MNIST, and CIFAR-20 experiments, the weight decay was set as 0.005,  $1e-05$ , and  $1e-07$ , respectively. Since we did not split the validation data in class-prior shift experiments, we set the  $\alpha$  in (5) as 0.5.

## C Supplementary experimental results

In this section, we present supplementary experimental results, including the histogram plots of the learned O-SVM score, visualizations of convolution kernels for all methods under label noise, additional experimental results for case (iv), and the summary of classification accuracy.

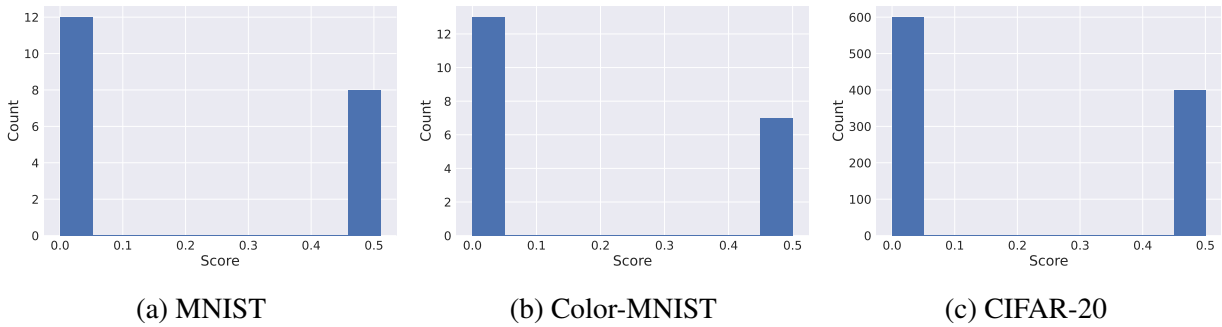


Figure 8: Histogram plots of the learned O-SVM score under support shift.

### C.1 On the learned O-SVM score

Figure 8 shows the histogram plots of the learned O-SVM score on MNIST, Color-MNIST, and CIFAR-20 under support shift. From the histogram plots, we observe that the score distribution consisted of two peaks without overlapping; therefore, any value between the two peaks (e.g., 0.4) could be made as a threshold to split the validation data into two parts. If the score of validation data was higher than the threshold, then the data was identified as an (in-training) IT validation data; otherwise, it was an (out-of-training) OOT validation data.

After splitting the validation data,  $\alpha$  in (5) was estimated as the ratio of the sample size between the IT validation data and the whole validation data, i.e.,  $\hat{\alpha} = n_{v1}/n_v$ . For example, in Figure 8a,  $\hat{\alpha} = \frac{8}{8+12} = 0.4$ , which equals to the true value in MNIST experiments. Similarly, it could be verified that  $\alpha$  in Figure 8b and 8c were also correctly estimated.

### C.2 Visualizations of convolution kernels under label noise

We further visualized the learned convolution kernels for all methods on Color-MNIST under 0.2 label noise. From Figure 9, we can see that the results aligned with the discussions about Figure 4. Previous IW or IW-like methods (i.e., Reweight, MW-Net, R-DIW, and DIW) only learned weights on the red channel, and Pretrain Val learned most weights on the red channel, which may cause the failure on the test data with green/blue color. Although Val only had weights on all colored channels, it may fail to learn useful data representation due to the limited sample size. Only GIW could successfully recover the weights on all channels while capturing the data representation.

### C.3 Additional experimental results for case (iv)

Here we present the empirical results under distribution-support shift on MNIST in case (iv). From Figure 10, we can see that GIW outperforms other methods by a large margin in case (iv) under both label-noise and class-prior-shift settings.

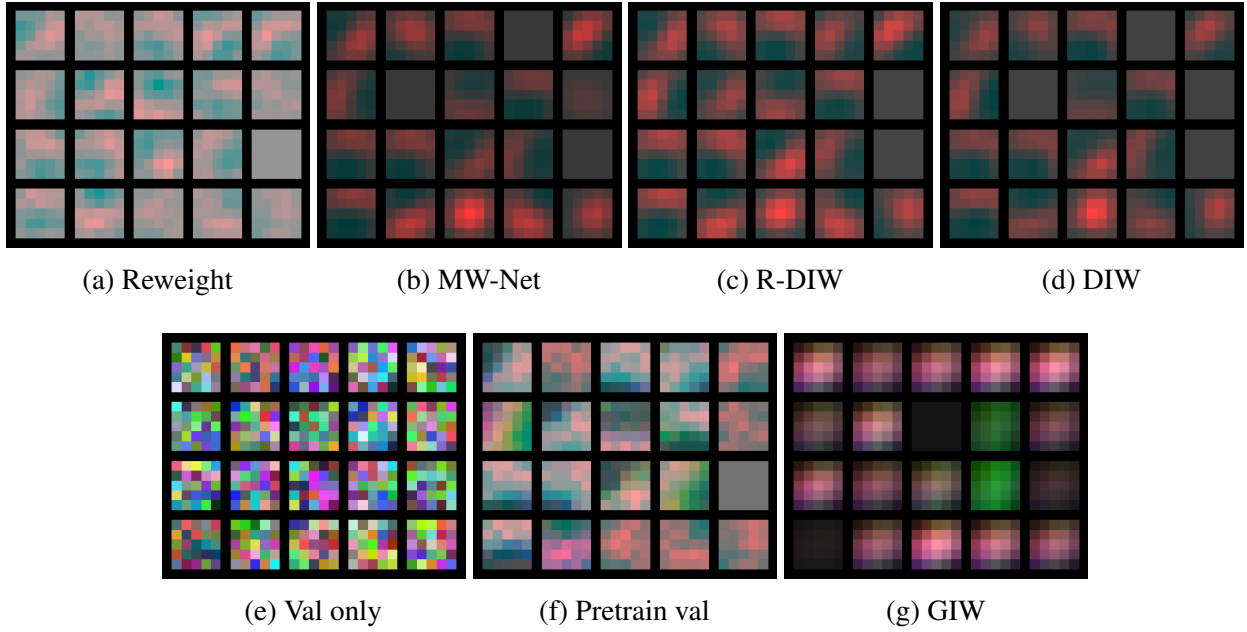


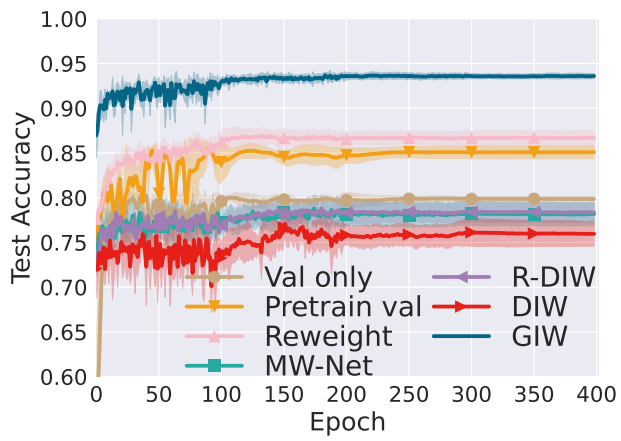
Figure 9: Visualizations of the learned convolution kernels on Color-MNIST under 0.2 label noise.

Table 2: Mean accuracy (standard deviation) in percentage on MNIST, Color-MNIST, and CIFAR-20 over the last ten epochs under support shift in case (iii) (5 trials). Best and comparable methods (paired  $t$ -test at significance level 5%) are highlighted in bold. This result corresponds to Figure 3.

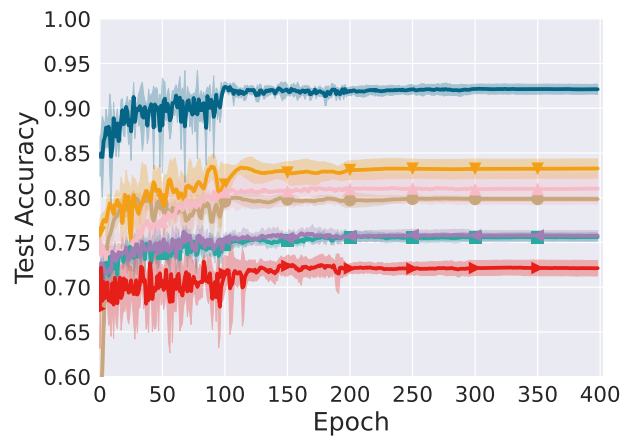
Data	Case	Val only	Pretrain val	Reweight	MW-Net	R-DIW	DIW	GIW
MNIST	(iii)	78.94 (0.99)	88.31 (1.02)	82.03 (0.13)	82.17 (0.32)	81.73 (0.42)	80.53 (1.23)	<b>95.17 (0.18)</b>
MNIST	(iv)	79.86 (0.26)	86.25 (0.95)	77.78 (0.91)	76.73 (0.63)	77.11 (0.63)	75.11 (1.43)	<b>91.23 (0.74)</b>
Color-MNIST	(iii)	31.19 (0.65)	80.40 (3.62)	38.39 (1.03)	39.26 (0.01)	39.28 (0.03)	39.50 (0.18)	<b>94.01 (0.17)</b>
CIFAR-20	(iii)	28.61 (0.66)	42.79 (0.41)	56.17 (0.29)	57.90 (0.18)	58.02 (0.35)	55.78 (0.34)	<b>59.68 (0.45)</b>

#### C.4 Summary of classification accuracy

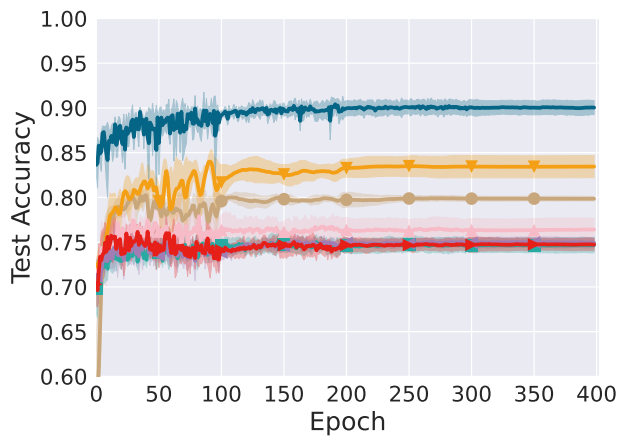
Table 2 and Table 3 present the mean accuracy (standard deviation) in percentage on MNIST, Color-MNIST, and CIFAR-20 over the last ten epochs under support shift and support-distribution shift, respectively. Table 2 and Table 3 correspond to Figure 3 and Figure 5. Table 4 shows the summary of the additional results in case (iv) on MNIST, corresponding to Figure 10.



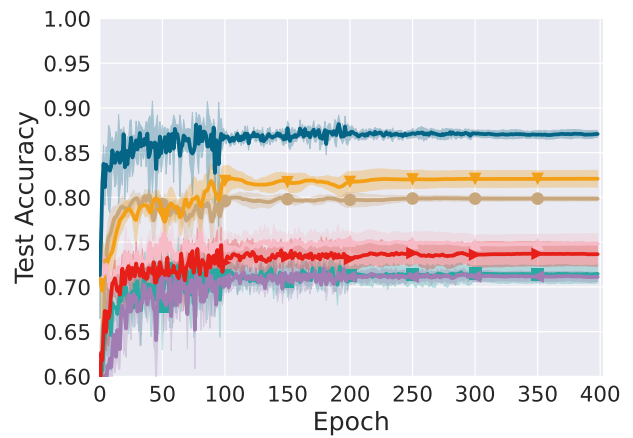
(a) Label noise 0.2



(b) Label noise 0.4



(c) Class-prior shift 10



(d) Class-prior shift 100

Figure 10: Results on MNIST in case (iv) under distribution-support shift (5 trails).

Table 3: Mean accuracy (standard deviation) in percentage on MNIST, Color-MNIST (C-MNIST for short), and CIFAR-20 over the last ten epochs under support-distribution shift in case (iii) (5 trials). Best and comparable methods (paired  $t$ -test at significance level 5%) are highlighted in bold. LN/CS is short for label noise/class-prior shift. This result corresponds to Figure 5.

Data	Shift	Val only	Pretrain val	Reweight	MW-Net	R-DIW	DIW	GIW
MNIST	LN 0.2	78.94 (0.99)	86.34 (0.77)	89.28 (0.64)	82.29 (0.80)	82.70 (0.76)	80.12 (2.90)	<b>94.79 (0.28)</b>
	LN 0.4	78.94 (0.99)	85.43 (0.97)	84.73 (1.27)	80.92 (0.52)	81.19 (0.39)	79.00 (0.33)	<b>93.57 (0.49)</b>
	CS 10	78.94 (0.99)	86.43 (0.71)	80.99 (0.67)	79.76 (0.60)	80.15 (0.38)	79.73 (0.38)	<b>93.49 (0.35)</b>
	CS 100	78.94 (0.99)	84.54 (1.61)	80.65 (0.71)	77.06 (0.71)	76.53 (0.45)	78.58 (0.96)	<b>91.41 (0.64)</b>
C-MNIST	LN 0.2	31.19 (0.65)	60.21 (4.47)	30.82 (1.04)	40.00 (0.44)	38.25 (0.46)	38.04 (1.83)	<b>90.99 (0.55)</b>
	LN 0.4	31.19 (0.65)	57.13 (5.48)	27.26 (0.41)	39.98 (0.06)	39.08 (0.02)	39.02 (0.50)	<b>90.14 (0.98)</b>
	CS 10	31.22 (0.69)	87.63 (1.97)	38.61 (0.62)	39.16 (0.19)	39.15 (0.19)	39.18 (0.19)	<b>94.82 (1.41)</b>
	CS 100	31.22 (0.69)	79.70 (3.29)	37.70 (0.21)	36.81 (0.10)	36.75 (0.17)	36.98 (0.23)	<b>88.08 (1.22)</b>
CIFAR-20	LN 0.2	28.74 (0.68)	40.35 (0.19)	48.41 (0.62)	45.36 (0.28)	45.46 (0.44)	46.84 (0.43)	<b>50.23 (0.71)</b>
	LN 0.4	28.74 (0.68)	37.95 (0.53)	41.02 (0.40)	33.02 (0.41)	32.90 (0.26)	36.69 (0.34)	<b>46.73 (0.80)</b>
	CS 10	28.45 (0.27)	37.31 (0.28)	42.25 (0.68)	44.96 (0.21)	45.19 (0.20)	39.68 (0.14)	<b>49.13 (0.28)</b>
	CS 100	28.45 (0.27)	36.55 (0.29)	31.95 (0.77)	34.66 (0.28)	34.87 (0.12)	26.39 (1.05)	<b>41.44 (1.90)</b>

Table 4: Mean accuracy (standard deviation) in percentage on MNIST over the last ten epochs under support-distribution shift in case (iv) (5 trials). Best and comparable methods (paired  $t$ -test at significance level 5%) are highlighted in bold. LN/CS means label noise/class-prior shift. This result corresponds to Figure 10.

Shift	Val only	Pretrain val	Reweight	MW-Net	R-DIW	DIW	GIW
LN 0.2	79.86 (0.26)	85.08 (0.71)	86.69 (0.80)	78.16 (1.30)	78.36 (1.08)	75.96 (1.39)	<b>93.58 (0.29)</b>
LN 0.4	79.86 (0.26)	83.26 (1.08)	81.01 (1.73)	75.60 (0.49)	75.76 (0.56)	72.12 (0.86)	<b>92.12 (0.55)</b>
CS 10	79.86 (0.26)	83.44 (1.24)	76.41 (1.28)	74.67 (0.84)	74.94 (0.59)	74.75 (0.69)	<b>90.04 (0.82)</b>
CS 100	79.86 (0.26)	82.09 (0.93)	74.84 (1.10)	71.42 (0.99)	71.11 (0.54)	73.66 (1.32)	<b>87.05 (0.42)</b>